Impact Behavior of Graphite/Epoxy Simulated Fan Blades

T. S. Cook*
Southwest Research Institute, San Antonio, Texas
and
J. L. Preston Jr.†
United Technologies, South Windsor, Conn.

An investigation of the response of the graphite/epoxy material Modmor II/PR-286 to foreign object impact was made by impacting spherical projectiles of gelatin, ice, and steel on static simulated blade specimens. Visual and metallographic inspection revealed three damage mechanisms: penetration, leading-edge bending failure, and stress wave delamination and cracking. The impact damage extents in the simulated blade tests were compared to the results of flat panel tests conducted earlier. It was found that the results of the different specimen tests could be correlated on the basis of two dimensionless parameters. This method of analysis shows potential for scaling results for small specimens with simple geometry to full-scale blades.

Introduction

EXPERIMENTS have shown that turbine engines with fan blades made of advanced fiber-reinforced composite materials have superior performance when compared to engines with blades of conventional monolithic materials. This superiority results from the composite material's unique combination of low weight with high specific strength and modulus. However, tests have shown that composite blades suffer an unacceptable degree of damage in collision with foreign objects. Since turbine engines ingest such diverse media as birds, hail, and gravel during normal flight operations, the lack of impact strength has prevented designs from utilizing the advantages of fibrous composites in designing first-stage turbine blades.

The investigation of the response of a structure to suddenly applied loads is an old field of study, but since the development of composite materials is relatively recent, most previous efforts have been directed at homogeneous elastic media. (A comprehensive review of the classical methods of analysis of impact is given by Goldsmith in Ref. 1.) With the development of composite materials for structural applications, it has become necessary to investigate the behavior of these materials under impact loads.[2-11] Analytical attempts to assess the influence of the composite on impact behavior have included the effect of laminated plates and anisotropy.[2-4] Other investigators have combined experimental Charpy impact studies with simple models to determine the importance of volume fraction and other composite parameters.[5-6] Investigations involving full-scale blades have been performed in the laboratory and in numerical studies.[7-8]

Previously, Preston and Cook used spherical projectiles to investigate the effect of projectile character and velocity on the damage done to flat plates in normal impacts.[9] These tests shed considerable light on the failure modes of the graphite epoxy composites but the lack of a scaling factor makes it difficult to determine if, in fact, the mechanisms observed in these tests are the same ones observed in an actual structure. To overcome this objection, the next phase of the investigation utilized a simulated blade to begin to evaluate the effects of target geometry. Initially an air cannon was used to fire spherical projectiles of gelatin, ice, and steel at a static test specimen. A second set of tests employed a rotating arm rig to determine the effect of the centrifugal stress on the impact response. The spin tests were also used to evaluate the reduction in impact damage by a leading edge shield by adding a stainless steel insert to the leading edge of some of the blades.

Specimen Preparation

The simulated blade specimens used in this program were constructed of Modmor II/PR-286‡ graphite/epoxy composite. Physical properties of the composite material are given in Ref. 9. The specimens were molded at 411-422 K (280-300°F) for 2 h, followed by a 16-h oven post cure at 422 K (300°F). The mold was pressed to stops to achieve an average cured ply thickness of 0.013 cm per ply and to insure dimensional accuracy at the leading and trailing edge to within ±0.008 cm. All specimens had a 57±2% by volume fiber content with densities ranging from 1.49 to 1.53 g/cc. The specimen configuration used was a cantilevered double-tapered simulated blade of constant cross section, as shown in Fig. 1. Fiberglass doublers were bonded to the blade and used for gripping purposes.

The specimens were constructed using two "core-and-shell" ply configurations. The standard configuration, $[(\pm 45)_2/0_{20}/(\mp 45)_2]$ (nominal), used four 45-deg plies as the shell. The second layup was designed to improve the chordwise stiffness by alternating 0- and 90-deg plies in the outer shell plies; the layup used was $[(90,\ 0)_4/0_{12}/(0,\ 90)_4]$ (nominal). Since the diamond cross-section panels had varying numbers of ply layers depending on the distance from the leading edge, these nominal layups were the configurations at quarter-chord. Starting with two full-width outer plies on both outer surfaces, the nominal quarter-chord compositions were maintained by varying the widths of the remaining plies.[10]

Presented as Paper 77-365 at the AIAA/ASME 18th Structures, Structural Dynamics, and Materials Conference, San Diego, Calif., March 21-23, 1977; submitted March 21, 1977; revision received Dec. 13, 1977.

Index categories: Structural Durability (including Fatigue and Fracture); Structural Composite Materials.

*Senior Engineer, Department of Materials Sciences.

†Senior Engineer, Power Systems Division.

‡Modmor II graphite fiber is a product of Hercules, Inc.; PR-286 epoxy thermosetting resin is a proprietary product of the 3M Co.

Static Specimen Tests

To simulate the objects encountered by turbine engines in operation, steel, ice, and gelatin were chosen as representative of metallic objects, hail, and birds, respectively. The projectiles were 1.27-cm-diam spheres for ice and gelatin, and 0.64-cm-diam spheres for steel, with all projectiles weighing approximately 1 g. An air cannon was used to propel the spheres at an average velocity of 274 m/s. Projectile speed was measured by using two light beams to time the projectile over a measured distance. Impact took place approximately 11.4 cm from the gripped end at angles of 0, 15, and 30 deg with respect to the chordwise center plane of the specimens.

The significance of the parameters was determined by the extent of target damage as measured by ultrasonic C-scan.

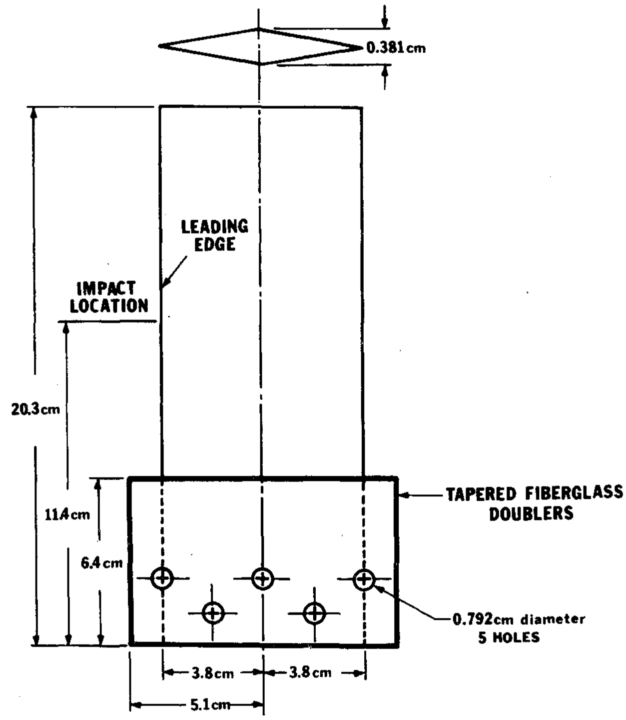

Fig. 1 Test specimen.

Damage extent percentages were obtained by ratioing the measured damaged area by the total area of the specimen. Areas where the entire thickness of a specimen were removed were also measured and were expressed as a percentage of material removed based upon total area.

The parameters of projectile type, impact location and angle, and ply configuration were all significant in determining the extent of damage. The effects of projectile characteristics and impact angle and locations in impacting the 0, ±45 deg specimens are summarized in Table 1.

The steel projectiles caused measurable damage in the composite material in all impacts in all tests. Figure 2 shows typical damage to the composite simulated blades for the steel projectile. The steel projectile penetrated the composite specimens under all conditions, but the damage extents and material loss were higher for the 15-deg quarter-chord and the 0-deg leading-edge shots than in either the 15- or 30-deg impacts on the leading edge. Small areas of delamination of the back face plies were usually evident, and are visible in Fig. 2.

Leading-edge damage increased with increasing impact angle with the gelatin projectile. The gelatin projectiles caused no damage in the 0-deg impacts on the leading edge; the leading edge sliced the projectile into two pieces without the blade undergoing large deformation. Impacts at 15 and 30 deg on the leading edge caused local structural failures with resulting delamination and peeling of the rear face shell layers, as shown in Fig. 3. As would be expected, the 30-deg shots produced significantly more damage than the 15-deg impacts. No damage to the target was observed in the 15-deg impacts at the thicker quarter-chord location. Damage done to the blade specimens by the ice projectiles was similar to that done by the gelatin, although slightly less severe.

To determine the effects of ply configuration, 1.27-cm-diam gelatin projectiles traveling at 274 m/s were fired against a standard $[(\pm 45)_2/0_{10}]_S$ (nominal) and a chordwise stiffened $[(90, 0)_4/0_6]_S$ (nominal) layup. Comparison of the results for 15-deg leading-edge impacts in Table 2 reveals an improvement in the impact resistance of the 0, 90-deg layup. The 0, ±45-deg layup suffered internal damage and lost material, whereas the 0, 90-deg layup was undamaged. Impact at 15-deg quarter-chord did not damage either specimen. Both the 90- and 45-deg specimens were found to be free of internal and external damage when sectioned and examined metallographically after 15-deg impacts at quarter-chord.

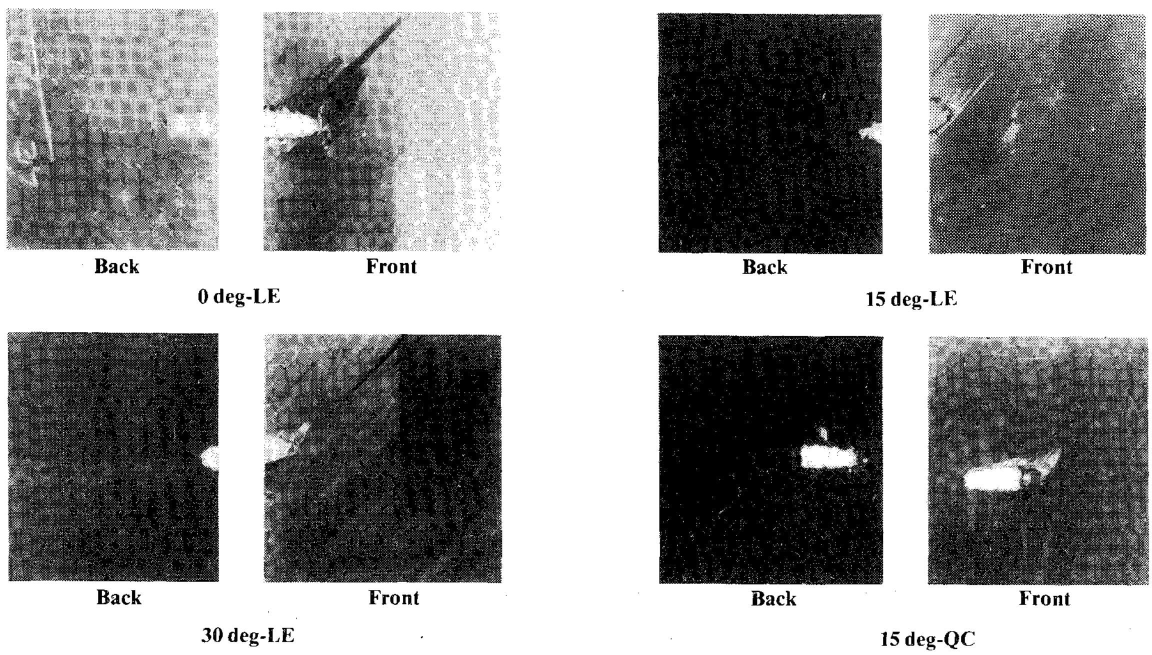

Fig. 2 Impact damage after 0.64-cm-diam steel impacts at 274 m/s.

Table 1 Effect of projectile characteristics, impact location, and angle of graphite/epoxy targets[a]

Projectile type	Diam., cm	Velocity, m/s	Impact angle, deg	Impact location	Material removal, %	Damage extent, %	Visual observation
Ice	1.27	274	0	LE	0	0	No visible damage.
Ice	1.27	278	0	LE	0	0	No visible damage.
Steel	0.64	274	0	LE	0.6	3.3	Leading edge penetrated to depth of 1.6 cm in chordwise direction.
Steel	0.64	274	0	LE	0	2.6	Glancing impact. 0.3 cm square portion of leading edge removed with fiber breakage and delamination visible along back side.
Gel.	1.27	272	0	LE	0	0	No visible damage.
Gel.	1.27	264	0	LE	0	0	No visible damage.
Ice	1.27	274	15	LE	0.4	2.6	1.2 cm long by 0.5 cm deep segment removed from leading edge. Delamination along back side.
Ice	1.27	277	15	LE	0	0.6	Delamination and fiber breakage on back side of leading edge.
Steel	0.64	274	15	LE	0.1	0.6	Leading edge penetrated to depth of 0.7 cm in chordwise direction.
Ice	1.27	285	30	LE	1.3	4.3	3.3 cm long by 0.7 cm deep segment removed from leading edge. Delamination on back side.
Ice	1.27	269	30	LE	0.7	4.9	1.0 cm square segment of leading edge removed. Delamination on back side.
Steel	0.64	274	30	LE	0.1	0.8	A 0.7 cm square segment of leading edge removed.
Steel	0.64	274	30	LE	0.6	1.0	Leading edge penetrated to depth of 1.0 cm in chordwise direction.
Gel.	1.27	282	30	LE	1.1	5.6	1.5 cm long by 0.9 cm deep segment removed from leading edge. Delamination on back side.
Gel.	1.27	292	30	LE	1.3	6.0	2 cm wide by 1 cm deep portion of leading edge removed.
Ice	1.27	274	15	QC	...	...	Ice failed to impact in proper location.
Ice	1.27	283	15	QC	0	0	No visible damage.
Steel	0.64	274	15	QC	0.4	4.9	A 0.5 cm wide by 0.9 cm chordwise hole at quarter-chord location. Lifting and delamination of back face plies.
Steel	0.64	274	15	QC	0.9	8.1	Leading edge intact. A 0.5 cm wide hole extends chordwise between 1.0 cm and 2.5 cm from leading edge. Delamination and ply lifting at back face.
Steel	0.64	274	15	QC	0.4	5.6	A 0.6 cm wide hole extends chordwise between 1.5 cm and 2.6 cm from leading edge. Delamination and ply lifting at back face.

[a] Modmor II/PR 286 – 0, ±45 deg layup.

Spin Impact Tests

The spin impact tests of nine simulated blades were designed to introduce effects of rotation and to evaluate the effect of a leading-edge protective shield on impact damage. The test parameters were essentially the same as for the static tests, except that all impacts occurred at 15 or 30 deg on the leading edge. The projectile velocity in all cases was 274 m/s. All specimens were tested in a chamber evacuated to 254 Torr to eliminate heating effects.

By providing improved resistance to deformation resulting from foreign object impact, a leading-edge shield can contribute significantly to improved impact resistance for a composite blade with a very thin leading edge. The shield used in these tests was constructed by removing the leading edge of blade to a chordwise depth of 0.84 cm over a 10.3 cm portion of the leading edge starting at a point 1.5 cm from the gripped end and replacing that by a 30-deg stainless steel insert covered by a stainless steel foil extending 2.5 cm back from the leading edge on both sides of the specimen. The entire leading-edge shield was then adhesively bonded to the blade, using Miller-Stephenson 907 epoxy adhesive.

Three composite specimens without shields were tested, one for each type of projectile. Although the rotation test specimens were not ultrasonically tested, the qualitative damage extents were comparable to the damage done in the air cannon tests. The three tests were to have been leading-edge impacts but the steel projectile struck the rotating blade slightly behind the leading edge and penetrated the specimen, leaving a relatively clean hole. The damage done by the ice and gelatin projectiles to the unprotected leading edge was similar in the static and dynamic tests. It appears that the effect of centrifugal force in these tests was negligible. However, it is difficult to generalize this result, since it is dependent on the geometry of the blade and these were relatively small blades. The effectiveness of the stainless steel shields was assessed in six impacts designed to duplicate a static test condition. Two steel projectiles were targeted for 15-deg leading-edge impacts. The first caused severe bending

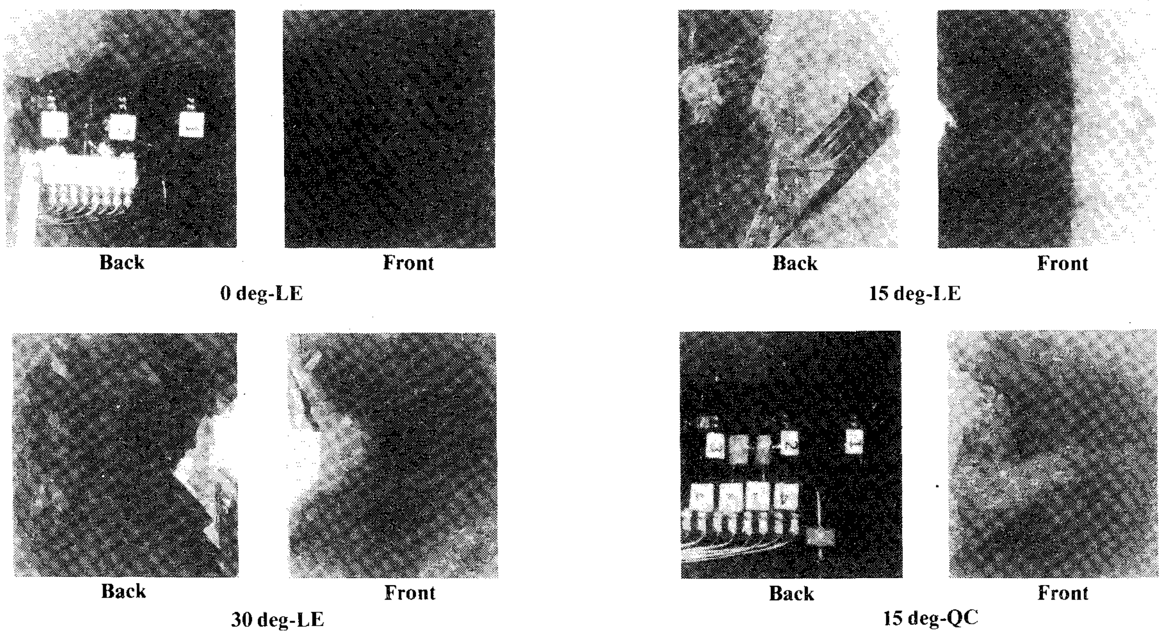

Fig. 3 Impact damage after 1.28-cm-diam gelatin impacts at 274 m/s.

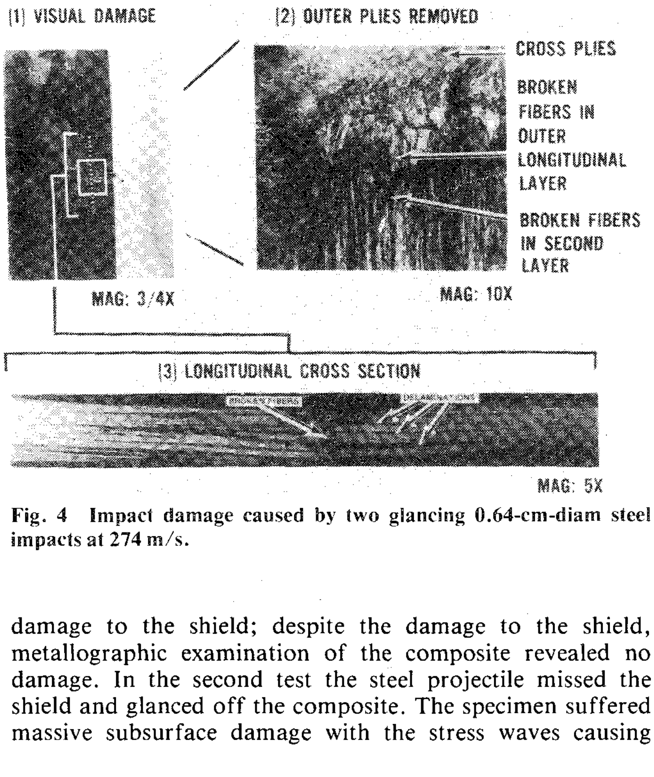

Fig. 4 Impact damage caused by two glancing 0.64-cm-diam steel impacts at 274 m/s.

damage to the shield; despite the damage to the shield, metallographic examination of the composite revealed no damage. In the second test the steel projectile missed the shield and glanced off the composite. The specimen suffered massive subsurface damage with the stress waves causing broken fibers and delaminations through the entire thickness as depicted in Fig. 4.

The leading-edge shields were more effective in protecting the composite against ice and gelatin projectiles. The blade was almost undamaged by the gelatin impacts; however, one of the shielded specimens exhibited slight debonding between the shield and the composite base. The shield provided complete protection for the composite against impacts by the ice. The only damage noted was a slight dent in the shield.

Results and Discussion

The impact damage observed in the test specimens could essentially be classified into local (or stress-controlled) damage, and structural (or deformation-controlled) damage. Specifically, local damage refers to those impacts in which the stresses generated in the target exceed the strength of the target material. This damage may be either direct with the contact stresses exceeding the compressive, tensile, or shear strength of the material, and allowing the projectile to penetrate the target, or the damage may be stress-wave induced. The latter results from reflected tensile waves producing subsurface delamination and cracking. All the impacts with the steel projectiles caused local damage; all but one of the projectiles penetrated the blades, regardless of the angle or location of impact. In the leading-edge impacts, the blades displayed very small areas of back face delamination with the damage confined to the immediate neighborhood of

Table 2 Effect of ply configuration for Modmor II/PR-286[a]

Ply configuration, deg	Projectile velocity, m/s	Impact location	Material removal, %	Damage extent, %	Visual observations
0, ±45	296	LE	0.4	1.2	1.2 cm long by 0.3 cm deep segment removed from leading edge
0, ±45	274	LE	0.1	1.1	0.7 cm long by 0.4 cm deep segment removed from leading edge
0, ±45	260	QC	0	0	No visible damage
0, ±45	283	QC	0	0	No visible damage
0, 90	266	LE	0	0	No visible damage
0, 90	291	LE	0	0	No visible damage
0, 90	273	QC	0	0	No visible damage
0, 90	292	QC	0	0	No visible damage

[a] All impacts with 1.27-cm-diam gelatin at an angle of 15 deg.

the hole. This indicated that the hole was caused by shearing of the fibers with relatively little deformation. The one steel impact displaying stress-wave damage was also classed as local damage as there was little permanent deformation despite the massive internal cracking produced by the impact.

The alternate damage mode, structural damage, occurs when the contact stresses are not sufficiently high to cause penetration but the projectile does possess enough momentum to produce target damage. In this case, the projectile-target contact time is longer so that the rate of transfer of momentum from the projectile to the target is lower; instead of the contact pressure building rapidly to a peak value and causing penetration, the longer contact time gives the impacting bodies time to deform and to distribute the impact load. However, if projectile momentum is high enough, the resulting target deformation can exceed the ductility of the composite and cause structural failure. For example, a leading-edge impact can produce sufficiently high bending strains to exceed the failure strain of the composite and cause the loss of a section of the leading edge. The same damage mode exists on a larger scale when the projectile strikes a thicker section of the blade; a gross structural bending failure can occur at either the point of impact or the attachment point.

From calculations based on the Hertz impact model the contact time for the ice and gelatin impacts was calculated to be approximately four times as long as for the steel projectiles.[9] The longer contact time and the previous experience with the flat panel impacts led to expectation that the damage response of the blade to ice and gelatin edge impacts would be structural rather than penetration. The experiments confirmed this, showing that these projectiles removed more material than did the steel; they also had larger ultrasonic damage extents. The structural failure of the leading edge was due to the bending strains generated in this thin section. The impacts of these projectiles at quarter-chord produced no damage since the structure at quarter-chord was thick enough to prevent the generation of large deformations. The advantage in impact strength shown by the 90-deg layup and the blades with edge shields is basically due to the increased leading-edge stiffness of these blades. The leading edges of the simulated blades are very thin and, as a result, develop large strains under relatively small loads. Hence, any modification that increases the chordwise stiffness of the leading edge will be beneficial.

A similar argument applies to the blades protected with the stainless steel inserts when the projectiles are gelatin or ice. However, as has been pointed out, impacts with hard bodies produce local damage and the stiffness is not as much of a factor in this type of damage. Rather it is the strength of the steel inserts that enables it to prevent failure of the leading edge. It must, however, be emphasized that since the impacts are on very thin leading edges, the increases in FOD resistance provided by these two modifications will not necessarily be reflected in thicker or blunter leading edges.

In previous experiments with foreign objects, the resulting damage has often been correlated on the basis of either projectile velocity or energy.[12] Although this is adequate for a given projectile material, current research clearly indicates that velocity (or energy) is unable to correlate damage due to different projectile types. For example, in the determination of damage thresholds for Modmor II/PR-286, 1.27 cm steel projectiles with a velocity of 33 m/s (3.7 joules) showed signs of penetration, whereas the same size ice projectile at 317 m/s (49.7 joules) gave no indication of penetration.[9] The contact pressure generated by the steel was sufficient to produce penetration, whereas the ice was not, despite the order of magnitude difference in impact energies. Thus, it is impossible to compare different projectiles that have impacted the same structure and, more importantly, it is very difficult to utilize the behavior of small specimens to predict the response of actual structures.

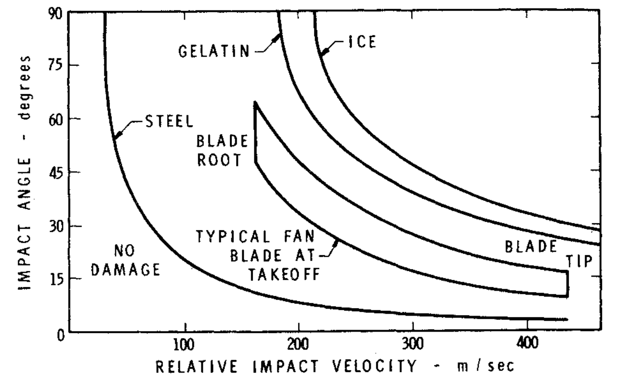

Fig. 5 Damage threshold as a function of relative velocity and impact angle for gelatin, ice, and steel projectiles.

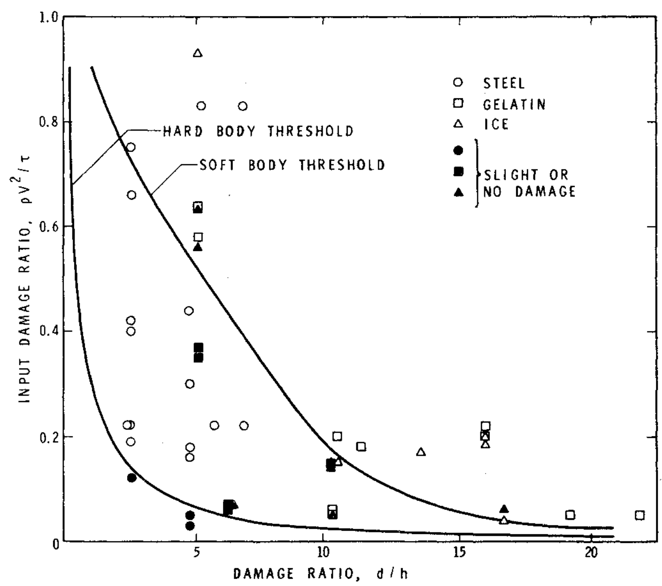

Fig. 6 Summary of impact damage results.

Figure 5 shows the relationship between the operating conditions of a typical fan blade at takeoff condition and the threshold of damage for the Modmor II/PR-286 composite. This result is developed from the flat panel work in Ref. 9 and applies only to the threshold for local damage. The figure shows that the threshold for steel projectiles completely envelops the blade while the thresholds for ice and gelatin projectiles lie above this blade. According to this estimate, the steel projectiles constitute the main hazard for FOD.

For birds and ice, however, the major concern about FOD is structural rather than local damage. In an effort to combine the two types of damage, the results of both the simulated blade and flat panel impacts were correlated in terms of the dimensionless parameters, $\rho V^2/\tau$ vs d/h, where

ρ = projectile mass density
V = projectile velocity
τ = target strength
d = characteristic projectile length
h = characteristic target length

Figure 6 shows that the damage parameter groups the damage observations into impacts that produce local (penetration and/or stress waves) and structural (leading-edge or root bending) damage depending on d/h. For a given d/h, increasing levels of $\rho V^2/\tau$ indicate increasing levels of damage; decreasing levels of $\rho V^2/\tau$ reach a damage threshold, below which no damage is observed.

In Figure 6, the different types of damage are accounted for through the use of the appropriate target strength, τ. The open points are complete local or flexural failure, whereas the solid points indicate moderate delamination or no damage at all. The lines indicate the approximate border of regions of severe damage for the hard (steel) and soft (gelatin, ice) projectiles. At very high velocities, small projectiles of both hard and soft material can cause penetration damage. Conversely, projectiles of both types that are large relative to the target can cause flexural failure at low speed. In the mid-range of d/h values, the steel projectiles have a very low damage threshold and penetrated the simulated blade target at low velocities. Over this d/h range, the gelatin projectile impacts with the simulated blades caused either delamination or local structural failure; the tendency to produce structural damage increased as d/h increased, i.e., the impact moved from the thicker quarter-chord location to the thin leading edge. The effect of the ice projectiles on the graphite/epoxy target is similar but high-speed photographs of ice projectiles showed some weight loss during flight; this may partially account for the consistently lower levels of damage caused by comparable ice and gelatin impacts.

Conclusions

The results of this experimental program demonstrate the necessity for separating the impact damage in composite bodies into regimes in order to isolate the primary failure mechanism. This study has classed the FOD as local or structural damage; this has strong implications for future material development programs. The conditions that determine the response to impact are highly specimen dependent, i.e., specimen ply lay-up, thickness, and gripping, etc., are all important parameters that determine not only the extent of damage, but also whether the damage is local or structural. The inability to correlate the damage done in small laboratory specimens to that observed in full-scale blades has been a barrier to the use of small specimens for parametric studies. The damage parameter developed in this study shows potential of being a scale factor that will allow experiments to be performed on small specimens with simple geometries and allow the results to be applicable to full-scale blades.

Acknowledgment

The work conducted in this program was supported by the National Aeronautics and Space Administration under contract No. NAS3-15568 administered by the Lewis Research Center. The authors would like to thank Howard Rulnick for his help in specimen preparation and data reduction.

References

[1] Goldsmith, W., *Impact*, Edward Arnold Ltd., London, 1960.

[2] Chen, W. T. and Engel, P. A., "Impact and Contact Stress Analysis in Multilayer Media," *International Journal of Solids Structures*, Vol. 8, Nov. 1972, p. 1257.

[3] Greszczuk, L. B., "Response of Isotropic and Composite Materials to Particle Impact," *Foreign Object Impact Damage to Composites*, American Society for Testing and Materials, ASTM STP 568, 1975, pp. 183-211.

[4] Sun, C. T. and Chattopadhyay, S., "Dynamic Response of Anisotropic Laminated Plates Under Initial Stress to Impact of a Mass," *Journal of Applied Mechanics, Trans. ASME,* Vol. 97, Sept. 1975, p. 693.

[5] Novak, R. C. and DeCrescente, M. A., "Impact Behavior of Unidirectional Resin Matrix Composites Tested in the Fiber Direction," *Composite Materials: Testing and Design* (*Second Conference*), American Society for Testing and Materials, ASTM STP 497, 1972, p. 311.

[6] Chamis, C. C., Hanson, M. P., and Serafine, T. T., "Impact Resistance of Unidirectional Composites," *Composite Materials: Testing and Design* (*Second Conference*), American Society for Testing and Materials, ASTM STP 497, 1972, p. 324.

[7] Premont, E. J. and Stubenrauch, K. R., "Impact Resistance of Composite Fan Blades," NASA CR-134515, May 1973.

[8] Fulton, G. B., "Design and Qualification of Foreign Object Damage Resistant Turbofan Blades," AIAA Paper 75-1313, Anaheim, Calif., 1975.

[9] Preston, J. L. Jr. and Cook, T. S., "Impact Response of Graphite-Epoxy Flat Laminates Using Projectiles that Simulate Aircraft Engine Encounters," *Foreign Object Impact Damage to Composites*, American Society for Testing and Materials, ASTM STP 568, 1975, p. 49.

[10] Friedrich, L. A., "Impact Resistance of Hybrid Composite Fan Blade Materials," NASA CR-134712, May 1974.

[11] Friedrich, L. A. and Preston, J. L. Jr., "Impact Resistance of Fiber Composite Blades Used in Aircraft Turbine Engines," NASA CR-134502, May 1973.

[12] Suarez, J. A. and Whiteside, J. B., "Comparison of Residual Strength of Composite and Metal Structures After Ballistic Damage," *Foreign Object Impact Damage to Composites*, American Society for Testing and Materials, ASTM STP 568, 1975, pp. 72-91.